

## Structure of Fasciculin 2 from Green Mamba Snake Venom: Evidence for Unusual Loop Flexibility

MARIE-HÉLÈNE LE DU,<sup>a†</sup> DOMINIQUE HOUSSET,<sup>a</sup> PASCALE MARCHOT,<sup>b</sup> PIERRE E. BOUGIS,<sup>b</sup> JORGE NAVAZA<sup>c</sup> AND JUAN CARLOS FONTECILLA-CAMPS<sup>a\*</sup>

<sup>a</sup>Laboratoire de Cristallographie et Cristallogénèse des Protéines, Institut de Biologie Structurale J.-P. Ebel, CEA - CNRS, 41, avenue des Martyrs, 38027 Grenoble CEDEX 1, France, <sup>b</sup>Laboratoire de Biochimie, CNRS, URA 1455, Université d'Aix-Marseille II, Faculté de Médecine, Secteur nord, boulevard Pierre Dramard, 13916 Marseille CEDEX 20, France and <sup>c</sup>Laboratoire de Physique, UPR 180, Centre d'Etudes Pharmaceutiques, 92290 Chatenay Malabry, France

(Received 7 November 1994; accepted 7 June 1995)

### Abstract

The crystal structure of the snake toxin fasciculin 2, a potent acetylcholinesterase inhibitor from the venom of the green mamba (*Dendroaspis angusticeps*), has been determined by the molecular-replacement method, using the fasciculin 1 model and refined to 2.0 Å resolution. The introduction of an overall anisotropic temperature factor improved significantly the quality of the electron-density map. It suggests, as it was also indicated by the packing, that the thermal motion along the unique axis direction is less pronounced than on the (*ab*) plane. The final crystallographic *R* factor is 0.188 for a model having r.m.s. deviations from ideality of 0.016 Å for bond lengths and 2.01° for bond angles. As fasciculin 1, fasciculin 2 belongs to the three-finger class of *Elapidae* toxins, a structural group that also contains the  $\alpha$ -neurotoxins and the cardiotoxins. Although the two fasciculins have, overall, closely related structures, the conformation of loop I differs appreciably in the two molecules. The presence of detergent in crystallization medium in the case of fasciculin 2 appears to be responsible for the displacement of the loop containing Thr9. This conformational change also results in the formation of a crystallographic dimer that displays extensive intermolecular interactions.

### 1. Introduction

Snake venoms from the *Elapidae* and *Hydrophidae* families contain complex mixtures of proteins some of which are potent toxins. One of the best studied groups of snake toxins is characterized by sharing a polypeptide fold first described for erabutoxin b (Low *et al.*, 1976). These molecules, that have molecular weights close to 7000 Da, can bind to their target with high affinity, have no catalytic function and are functionally diversified.

<sup>†</sup>Present address: Section of Biochemistry, Molecular and Cell Biology, 209 Biotechnology Building, Cornell University, Ithaca, NY 14853, USA.

Numerous crystallographic analyses (Low *et al.*, 1976; Tsernoglou & Petsko, 1976; Love & Stroud, 1986; Rees *et al.*, 1987; Betzel *et al.*, 1991; le Du, Marchot, Bougis & Fontecilla-Camps, 1992; Nickitenko, Michailov, Betzel & Wilson, 1993) as well as NMR studies (Labhardt, Hunziker-Kwik & Wüthrich, 1988; Steinmetz *et al.*, 1988; Laplante *et al.*, 1990; Yu, Lee, Chuang, Shei & Wang, 1990; Oswald *et al.*, 1991; Brown & Wüthrich, 1992; Zinn-Justin *et al.*, 1992; Golovanov, Lomize, Arseniev, Utkin & Tsetlin, 1993; O'Connell, Bougis & Wüthrich, 1993) have shown that all these toxins are constituted of a dense core typically containing four disulfide bridges, and of three long loops (called I, II and III) emerging from the core, like the three central fingers of a hand. They all contain two  $\beta$ -sheets: a three-stranded sheet comprising loop II and one segment of loop III, and a two-stranded one involving loop I. The best known members of the family are the short (62 amino acids, four disulfide bridges), and the long (70–80 amino acids, 4–5 disulfide bridges)  $\alpha$ -neurotoxins, which are known to bind to the nicotinic acetylcholine receptor (Changeux, Kasai & Lee, 1970; Endo & Tamiya, 1991).

An additional group of snake toxins of related amino-acid sequences and capable of inducing muscular fasciculations, the fasciculins, was originally described by Viljoen & Botes (1973). Fasciculins are 61 amino-acid residues long, and contain four disulfide bridges. They are very potent inhibitors of synaptic acetylcholinesterases ( $K_i \approx 10^{-10}$  M), and bind with a 1:1 stoichiometry to the so-called peripheral anionic site of the enzyme (Taylor & Lappi, 1975; Harvey, Anderson, Mbugua & Karlsson, 1984; Marchot, Khelif, Ji, Mansuelle & Bougis, 1993). Four fasciculins have been characterized to date: fasciculin 1 and 2 from the venom of *Dendroaspis angusticeps* (Rodriguez-Ithurralde, Silveira, Barbeito & Dajas, 1983), toxin C from the venom of *D. polylepis* (Joubert & Taljaard, 1978), and fasciculin 3 from the venom of *D. viridis* (Marchot *et al.*, 1993). Fasciculins 1 and 2 differ by only one residue: a tyrosine at position 47 in fasciculin 1 is replaced by an

asparagine in fasciculin 2. Although present in the venom of two different species, toxin C and fasciculin 3 appear to be the same protein (Marchot *et al.*, 1993). They differ from fasciculin 1 at three positions: 2 (Met to Ile), 15 (Thr to Lys) and 16 (Asn to Asp). The crystallographic analysis of fasciculin 1 (le Du *et al.*, 1992) confirmed that fasciculins have the three-finger type fold.

In order to determine the effect of the single substitution on the conformation of loop III, we initiated the crystallographic structure analysis of fasciculin 2. Surprisingly, when compared with fasciculin 1, fasciculin 2 shows unexpected large differences in the conformation of loop I.

## 2. Crystallization, data collection and processing

Fasciculin 2 was purified and crystallized as previously described (le Du, Marchot, Bougis & Fontecilla-Camps, 1989). The crystallization conditions of fasciculin 1 and fasciculin 2 were similar, except that the presence of  $\beta$ -octylglucoside was essential to obtain crystals of the latter. Fasciculin 2 crystals belong to the space group  $P4_12_12$  with unit-cell dimensions of  $a = b = 48.93$  and  $c = 82.18$  Å, and one molecule in the asymmetric unit ( $V_m = 3.64$  Å<sup>3</sup> Da<sup>-1</sup>, Matthews, 1968). Two sets of crystallographic data were collected at room temperature: one on a Xentronics/Siemens area detector, coupled to a

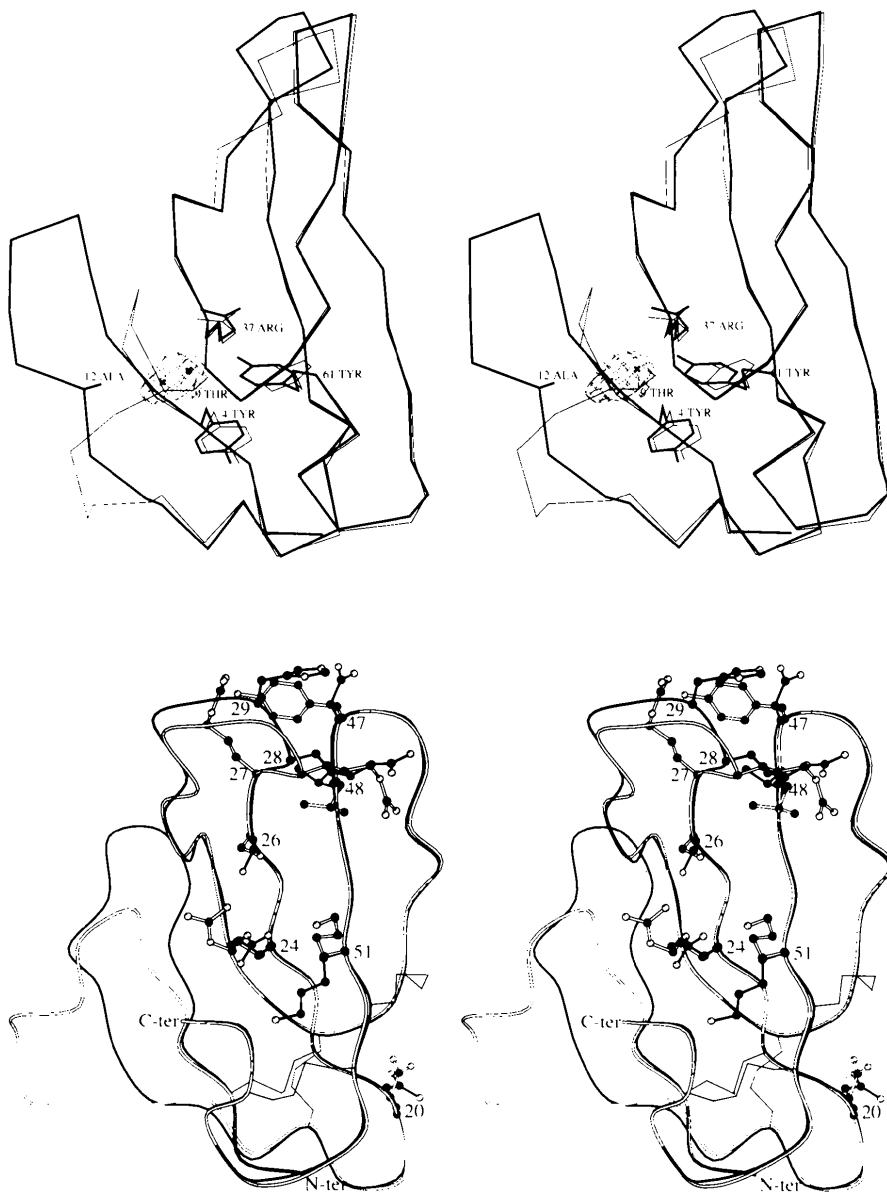


Fig. 1. Stereoscopic view of the superposed structures of fasciculin 2 (thick lines) and fasciculin 1. The vicinity of the 'detergent' molecule is shown in detail: in fasciculin 2, the two detergent atoms [for which the  $(2F_o - F_c)$  electron-density map contoured at the  $1\sigma$  level is shown] fill the hydrophobic pocket formed by Tyr4, Ala12, Tyr61 and Arg37. In fasciculin 1, the side chain of Thr9 (from loop I) fills this pocket, with the methyl group pointing towards the inside of the protein.

Fig. 2. Stereoscopic view of the superposed structures of fasciculin 2 (black lines) and fasciculin 1 (white ribbon) (produced with the program *MOLSCRIPT*, Kraulis, 1991). Ball-and-stick representation are for side chains with different conformation (where main-chain conformation is conserved). The stabilization of the side chain of residue 47 with Arg27 for fasciculin 1, and with His29 for fasciculin 2 is shown. Disulfide bridges are represented with thin solid lines.

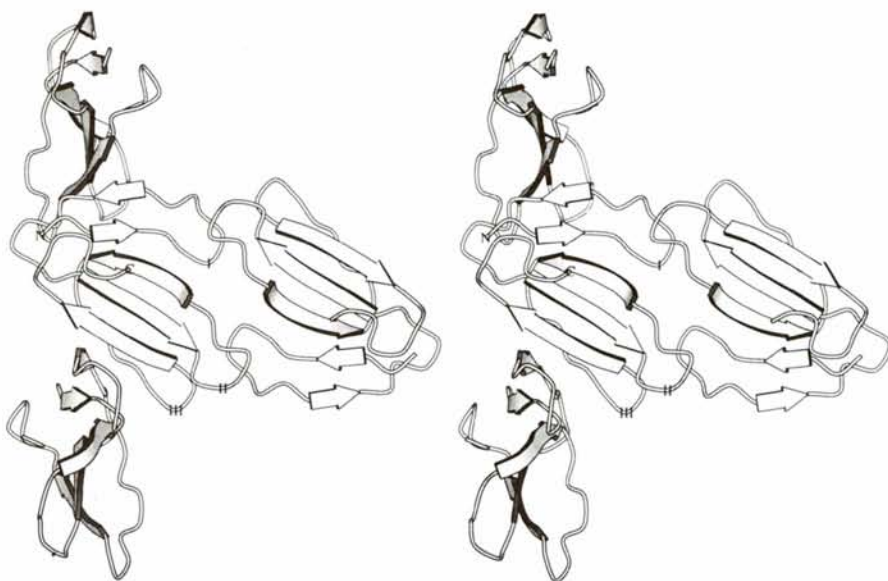


Fig. 3. Stereoscopic view of packing interactions in fasciculin 2 (produced with the program *MOLSCRIPT*, Kraulis, 1991): arrows are for  $\beta$ -strands, the reference molecule is in the center. Vertically ( $c$  axis), the intermolecular interactions form a continuous twisted  $\beta$ -sheet along the  $c$  axis. Horizontally (diagonal of  $a$  and  $b$  axes), the tight crystallographic dimer involves loop I and loop II.

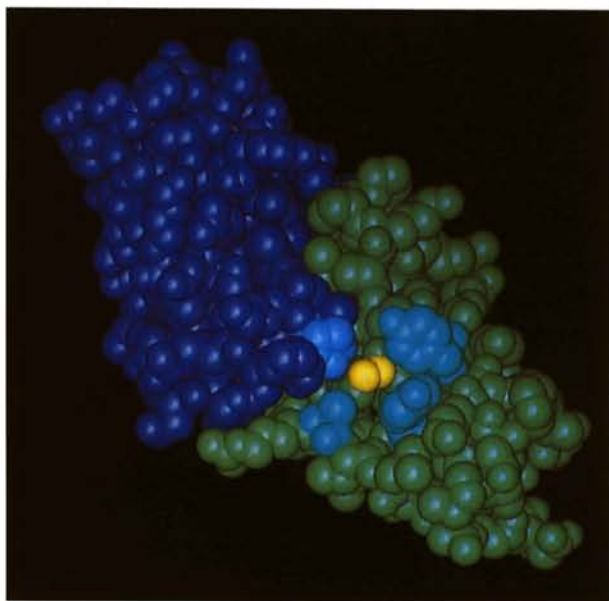


Fig. 4. CPK view of the crystallographic dimer of fasciculin 2, showing the putative detergent site at the interface. The reference molecule is green, the symmetry-related one, blue. The detergent atoms are represented in yellow, and the residues interacting with them are shown in light colours.

Rigaku RU200 X-ray generator ( $\lambda = 1.5418 \text{ \AA}$ ,  $\omega$  oscillation range of  $0.25^\circ$ ,  $2.3 \text{ \AA}$  resolution), another one at the W32 synchrotron beam port at LURE (Orsay, France), on a MAR Research image-plate area detector ( $\lambda = 0.90 \text{ \AA}$ ,  $\varphi$  oscillation range of  $1.5^\circ$ ,  $2.0 \text{ \AA}$  resolution). Data processing and internal scaling were carried out with *XENGEN* (Version 1.3, Howard *et al.*, 1987) for the former, and with *MOSFLM* (Version 4.3, Leslie,

1991), *ROTAVATA* and *AGROVATA* (CCP4 package, Collaborative Computational Project, Number 4, 1994) for the latter. The two data sets were then merged with the program *PROTEIN* (Steigemann, 1974, Table I).

### 3. Structure determination and refinement

The structure of fasciculin 2 was solved with the molecular-replacement program package *AMoRe* (Navaza, 1994), using the fasciculin 1 crystal structure (le Du *et al.*, 1992) as a search model. Both the rotation- and the translation-function searches resulted in well contrasted solutions. After rigid-body refinement of the fasciculin 1 model according to the molecular-replacement solution, the  $R$  factor and  $F$  correlation coefficient had values of 0.44 and 0.58, respectively, at  $2.5 \text{ \AA}$  resolution.

The fasciculin 2 model was refined in two steps using *X-PLOR* (Version 2.1, Brünger, 1990). Refinement was initiated with the  $2.3 \text{ \AA}$  resolution data set. Major corrections of the model were carried out interactively with the program *TURBO-FRODO* (Roussel & Cambillau, 1989). At this point, the model included 464 protein atoms and 25 water molecules, with an  $R$  factor of 0.219 for reflections with  $F \geq 2.5\sigma(F)$  in the  $6.0$  to  $2.3 \text{ \AA}$  resolution range. Once it became available, a  $2.0 \text{ \AA}$  resolution merged data set (including the data collected at LURE) was used. Regular positional refinement using *X-PLOR* was performed, alternating with solvent modeling steps using *PROTEIN* and *FRODO* (Jones, 1978). During the refinement process, in addition to the individual  $B$  factor, an overall anisotropic  $B$  factor was introduced resulting in a significant improvement of both the  $R$  factor and quality of the electron-density map. The final model includes 464 protein atoms and 57 solvent molecules. For the 6287 reflections between  $10.0$  and

Table 1. *Data collection and refinement statistics*

Resolution (Å)	Wavelength (Å)	No of measured reflections	No. of unique reflections	Redundancy	Completeness	$R_{\text{sym}}^*$
2.3	1.54	11690	4477	2.6	0.91	0.048
2.0	0.90	20878	6339	3.3	0.88	0.058
2.3 Å data set	Crystal-to-detector distance 120 mm, swing angle 10°					
2.0 Å data set	Crystal-to-detector distance 181 mm, swing angle 0°					
Merged data set	6363 reflections with $F \geq 2.5\sigma(F)$ in the resolution range 15.0–2.0 Å. $R_{\text{merge}}$ on intensities = 0.088					
Resolution (Å)	10.0–2.0 Å		[6287 reflections, $F \geq 2.5\sigma(F)$ ]			
$R$ factor	0.188					
Deviation from ideality						
Bonds (Å)	0.016					
Angles (°)	2.01					
Temperature factor						
Overall anisotropic $b$ factor (Å <sup>2</sup> )	$b_{11} = b_{22} = 0.081 (6.4)$		$b_{33} = -0.157 (-12.4)$			
Main chain (Å <sup>2</sup> )	25.0					
Side chain (Å <sup>2</sup> )	31.0					
Solvent (Å <sup>2</sup> )	50.6					

$$*R_{\text{sym}} = \frac{\sum_h \sum_l |I_{lh} - \langle I \rangle_h|}{\sum_h \sum_l \langle I \rangle_h}$$

2.0 Å resolution, the  $R$  factor of 0.188 and the geometry is of good quality (Table 1). The coordinates of the model have been deposited with the Protein Data Bank.\*

## 4. Results

### 4.1. Comparison with fasciculin 1

As it was expected, the overall topology of fasciculin 2 is similar to that of fasciculin 1. The program *ALIGN* (G. Cohen, in Satow, Cohen, Padlan & Davies, 1986) was used to superimpose the two fasciculins. After convergence, an r.m.s. difference of 0.29 Å is observed for 189 out of 244 pairs of atoms belonging to the main chain. The two molecules are very well superposed except for two regions: the  $\beta$ -turn at the distal part of loop II, with a distance of 2.0 Å between the respective Pro30  $\text{C}\alpha$ 's and, more dramatically, at loop I, with a maximal distance of 13.6 Å between corresponding Thr9 residues (Fig. 1). This change in loop I conformation introduces a connection between the two  $\beta$ -sheets of fasciculin 2, made of two hydrogen bonds between the main-chain atoms of His6 and Arg37, thus forming an effective five-stranded  $\beta$ -sheet. No main-chain conformational changes are observed in the vicinity of residue 47 (Tyr/Asp): only the side-chain interactions are different: the hydroxyl group of the tyrosine side-chain hydrogen bonds to the  $\text{N}^{\eta 2}$  atom of Arg27, while the asparagine points in the opposite direction, forming an hydrogen bond with His29 (Fig. 2). In the zones where the orientation of the main chain is well conserved, just a few side chains (located at the protein surface) have different conformations in the two toxins (Asn20, Arg24, Ser26, Arg28, Leu48 and Lys51, see Fig. 2). Among them, the

different orientation of Leu48 results from the Tyr47 to Asn47 change. Quite unexpectedly, the major differences between the two molecules are confined to loop I. Since, for this loop, the amino-acid sequences are identical in both fasciculins, in addition to a possible inherent flexibility, the structural differences can only be attributed to crystal packing and/or crystallization conditions.

### 4.2. Crystal packing

Comparison of the packing of fasciculin 1 and fasciculin 2 shows two remarkable features (Fig. 3): on the one hand, the intermolecular contacts along the  $c$  axis are very similar in the two fasciculins, in agreement with the similar  $c$ -axis lengths. Two main-chain–main-chain hydrogen bonds connect the second strand of the two-stranded  $\beta$ -sheet of one molecule to the third strand of the three-stranded  $\beta$ -sheet of a related one. This induces a continuous twisted  $\beta$ -sheet along the fourfold screw axis. Moreover, taking into account the overall anisotropic  $B$  factor, the thermal motion along the crystallographic  $c$  axes is similar in the two fasciculins. On the other hand, fasciculin 2 forms a tight dimeric interaction around a twofold axis, involving loops I and II. A fifth of the molecular surface (740 Å<sup>2</sup>) is, therefore, buried (Fig. 4). However, the fact that the dimer itself has no close contact with neighbouring molecules on the ( $ab$ ) plane explains the higher thermal motion in that plane.

### 4.3. Putative detergent site

During the refinement process, the residual ( $F_o - F_c$ ) electron-density map showed a large positive peak, in a hydrophobic pocket (Tyr4, Tyr61, Ala12, Pro30, Figs. 1 and 4) at the interface between the two molecules forming the crystallographic dimer (see above). For the purpose of the refinement, two O atoms were modeled in this density, with reciprocal van der Waals interactions

\* Atomic coordinates have been deposited with the Protein Data Bank, Brookhaven National Laboratory (Reference: 1FSC). Free copies may be obtained through The Managing Editor, International Union of Crystallography, 5 Abbey Square, Chester CH1 2HU, England (Reference: GR0416).

switched off to avoid mutual repulsion. However, although C, N or O atoms cannot be distinguished at this resolution, this density is unlikely to correspond to oxygen-containing molecules such as water (or a sulfate ion) since polar interactions should not be favored in this region (Wolfenden & Radzicka, 1994). Moreover the distance between this peak and the closest protein atoms is around 4 Å. Given the fact that the detergent appears essential for crystallization, the hydrophobic pocket could be occupied by part of the aliphatic chain of the  $\beta$ -octylglucoside molecule. Indeed, in the final model, the distance between the two modelled atoms is 1.65 Å, a value not too different from typical C—C bond distances.

### 5. Discussion

The analysis of the structure gives us some clues to explain the structural changes between fasciculin 1 and fasciculin 2. The fact that fasciculin 2 does not crystallize in the fasciculin 1 crystal form seems induced by the Tyr47 to Asn47 change. In fasciculin 1, Tyr47 interacts extensively with the rings of Tyr4 and Tyr61 of a symmetry-related mate. Since the side chain of the asparagine residue cannot establish the same hydrophobic interactions, Tyr47 appears to be essential for the molecular packing in the fasciculin 1 crystals.

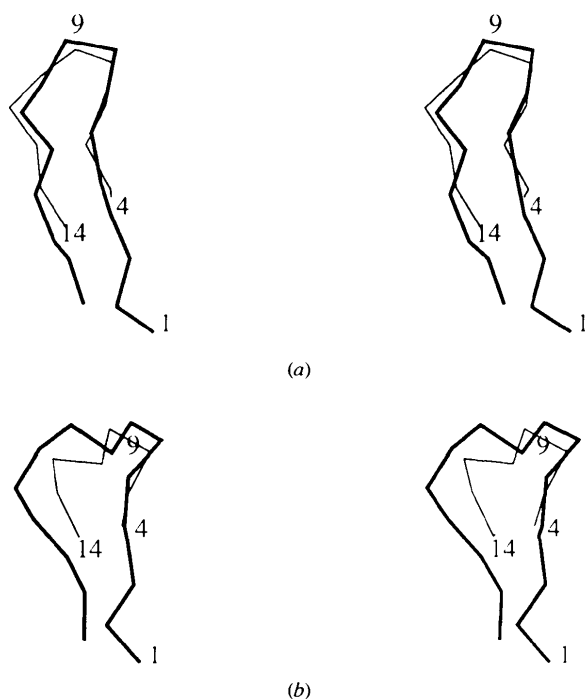


Fig. 5. Stereoscopic view of loop I. (a) Superposition of loop I fasciculin 2 (thick line, residues 4 to 14) on loop I from erabutoxin b. (b) Superposition of loop I from fasciculin 1 (thick line) on loop I from cardiotoxin.

The detergent seems to play a key role in the change of conformation observed for loop I. The conformation of this loop in fasciculin 1 makes the Thr9 side chain pack against the hydrophobic pocket, with the C $\alpha$  and C $\gamma$  of Thr9 being topologically equivalent to the two putative detergent atoms in fasciculin 2 (Fig. 1, this confirms the hydrophobic character of the pocket). By filling this pocket, the detergent allows loop I to adopt its extended conformation in fasciculin 2. This conformational change is essential for the strong dimeric packing interaction to take place (see above). The dimer appears as the elementary unit in the crystal, but there is no evidence for its existence in solution.

### 6. Concluding remarks

A structural difference such as the one observed for loop I is unusual among closely related small single-chain proteins. In fact, the differences between loop I conformations in the two fasciculins is the largest ever encountered among all the three-finger type snake toxins for which the refined three-dimensional structures are known. The conformations of loop I in fasciculin 2 and 1 are comparable to those of erabutoxin b (Smith, Cortfield, Hendrickson & Low, 1988, code 3EBX) (r.m.s. difference of 1.22 Å on C $\alpha$ 's, Fig. 5a) and cardiotoxin V $_4^{\text{II}}$  (Rees *et al.*, 1987) (r.m.s. difference of 1.78 Å on C $\alpha$ 's, Fig. 5b), respectively. This suggests that, regardless of the packing, the repertoire of possible conformations that the various loops of this class of snake toxins can assume may be limited (although their relative orientations can be significantly different).

Because only a small hydrophobic part of the detergent molecule seems to be visible in the electron-density maps, it is possible that other additives, such as alcohols or small amphipathic molecules, could have the same effect.

Very little is known about the regions of fasciculin responsible for the binding to and subsequent inhibition of acetylcholinesterase. From the analysis of mutants of mouse acetylcholinesterase, it appears that two tyrosines and one tryptophane (located on the peripheral anionic site of acetylcholinesterase) are essential for fasciculin binding (Radic *et al.*, 1994). Even though the structure of fasciculin 2 does not shed additional light on the binding of the toxin to the enzyme, the extreme flexibility of loop I may be of importance in this process.

The authors thank J. P. Benoît and R. Fourme for their assistance during data collection at the W32 beam port at LURE (Orsay, France).

### References

- Betzler, C., Lange, G., Pal, G. P., Wilson, K. S., Maelicke, A. & Saenger, W. (1991). *J. Biol. Chem.* **266**, 21530–21536.

- Brown, L. R. & Wüthrich, K. (1992). *J. Mol. Biol.* **227**, 1118–1135.
- Brünger, A. T. (1990). *X-PLOR Manual*, Version 2.1, Yale University, CT, USA.
- Changeux, J. P., Kasai, M. & Lee, C.-Y. (1970). *Proc. Natl Acad. Sci. USA*, **67**, 1241–1247.
- Collaborative Computational Project, Number 4 (1994). *Acta Cryst.* **D50**, 760–763.
- Du, M. H. le, Marchot, P., Bougis, P. E. & Fontecilla-Camps, J. C. (1989). *J. Biol. Chem.* **264**, 21401–21402.
- Du, M. H. le, Marchot, P., Bougis, P. E. & Fontecilla-Camps, J. C. (1992). *J. Biol. Chem.* **267**, 22122–22130.
- Endo, T. & Tamiya, N. (1991). *Snake Toxins*, edited by A. L. Harvey, pp. 165–222. Oxford: Pergamon Press.
- Golovanov, P., Lomize, A. L., Arseniev, A. S., Utkin, Y. N. & Tselin, V. I. (1993). *Eur. J. Biochem.* **213**, 1213–1223.
- Harvey, A. L., Anderson, A. J., Mbugua, P. M. & Karlsson, E. (1984). *J. Toxicol. Toxin Rev.* **3**, 91–137.
- Howard, A. J., Gilliland, G. L., Finzel, B. C., Poulos, T. L., Olhendorf, D. H. & Salemme, F. R. (1987). *J. Appl. Cryst.* **20**, 383–387.
- Jones, T. A. (1978). *J. Appl. Cryst.* **15**, 24–31.
- Joubert, F. & Taljaard, N. (1978). *S. Afr. J. Chem.* **31**, 107–110.
- Kraulis, P. J. (1991). *J. Appl. Cryst.* **24**, 946–950.
- Labhardt, A. M., Hunziker-Kwik, E. H. & Wüthrich, K. (1988). *Eur. J. Biochem.* **177**, 295–305.
- Laplante, S. R., Mikou, A., Robin, M., Guittet, E., Delsuc, M., Charpentier, I. & Lallemand, J. Y. (1990). *Int. J. Peptide Protein Res.* **36**, 227–230.
- Leslie, A. G. W. (1991). *Crystallographic Computing*, edited by D. Moras, A. D. Podjarny & J. C. Thierry, pp. 50–61. Oxford University Press.
- Love, R. A. & Stroud, R. M. (1986). *Protein Eng.* **1**, 37–46.
- Low, B., Preston, H. S., Sato, A., Rosen, L. S., Searl, J. E., Rudko, A. D. & Richardson, J. S. (1976). *Proc. Natl Acad. Sci. USA*, **73**, 2991–2994.
- Marchot, P., Khélif, A., Ji, Y.-H., Mansuelle, P. & Bougis, P. E. (1993). *J. Biol. Chem.* **268**, 12458–12467.
- Matthews, B. W. (1968). *J. Mol. Biol.* **33**, 491–497.
- Navaza, J. (1994). *Acta Cryst.* **A50**, 157–163.
- Nickitenko, A. V., Michailov, A. M., Betzel, C. & Wilson, K. S. (1993). *FEBS Lett.* **320**, 111–117.
- O'Connell, J. F., Bougis, P. E. & Wüthrich, K. (1993). *Eur. J. Biochem.* **213**, 891–900.
- Oswald, R. E., Sutcliffe, M. J., Bamberger, M., Loring, R. H., Braswell, E. & Dobson, C. M. (1991). *Biochemistry*, **30**, 4901–4909.
- Radic, Z., Duran, R., Vellom, D. C., Li, Y., Cervenansky, C. & Taylor, P. (1994). *J. Biol. Chem.* **269**, 11233–11239.
- Rees, B., Samama, J. P., Thierry, J. C., Gilbert, M., Fischer, J., Schweitz, H., Ladzunski, M. & Moras, D. (1987). *Proc. Natl Acad. Sci. USA*, **84**, 3132–3138.
- Rodriguez-Ithurralde, D., Silveira, L., Barbeito, L. & Dajas, F. (1983). *Neurochem. Int.* **5**, 267–274.
- Roussel, A. & Cambillau, C. (1989). *Silicon Graphics Geometry Partner Directory*, pp. 77–78. Mountain View, CA: Silicon Graphics.
- Satow, Y., Cohen, G. H., Padlan, E. A. & Davies, D. (1986). *J. Mol. Biol.* **190**, 593–604.
- Smith, J. L., Cortfield, P. W. R., Hendrickson, W. A. & Low, B. W. (1988). *Acta Cryst.* **A44**, 357–368.
- Steigemann, W. (1974). PhD thesis, Technische Universität München, Germany.
- Steinmetz, W. E., Bougis, P. E., Rochat, H., Redwine, O. D., Braun, W. & Wüthrich, K. (1988). *Eur. J. Biochem.* **172**, 101–116.
- Taylor, P. & Lappi, S. (1975). *Biochemistry*, **14**, 1989–1997.
- Tsernoglou, D. & Petsko, G. A. (1976). *FEBS Lett.* **68**, 1–4.
- Viljoen, C. C. & Botes, D. P. (1973). *J. Biol. Chem.* **218**, 4915–4919.
- Wolfenden, R. & Radzicka, A. (1994). *Science*, **265**, 936–937.
- Yu, C., Lee, C.-S., Chuang, L.-C., Shei, Y.-R. & Wang, C. Y. (1990). *Eur. J. Biochem.* **193**, 789–799.
- Zinn-Justin, S., Roumestand, C., Gilquin, B., Bontems, F., Ménez, A. & Toma, F. (1992). *Biochemistry*, **31**, 11335–11347.